Anatomy & Physiology: Current Research
ISSN: 2161-0940

da Silva Carvalho C et al., Anat Physiol 2014, 4:3
DOI: 10.4172/2161-0940.1000142

Research Article Open Access

Ultrastructural Morphometry of the Aortic Depressor Nerves and Extrinsic Renal Nerves: Similarities and Differences between Mice and Rats

da Silva Carvalho C[1], **Sato KL**[2,3], **Castania JA**[4], **Salgado HC**[4], **Nessler RA**[3] **and Fazan VPS**[1,3,5*]

[1]*Department of Neuroscience and Behavioral Neurosciences, School of Medicine of Ribeirao Preto, University of Sao Paulo, Ribeirao Preto, SP, Brazil*

[2]*Department of Physical Therapy, Federal University of Sergipe, Sergipe, SP, Brazil*

[3]*Central Microscopy Research Facility, The University of Iowa, Iowa City, IA, USA*

[4]*Department of Physiology, School of Medicine of Ribeirao Preto, University of São Paulo, Ribeirão Preto, SP, Brazil*

[5]*Department of Surgery and Anatomy, School of Medicine of Ribeirao Preto, University of São Paulo, Ribeirao Preto, SP, Brazil*

[*]**Corresponding author:** Valeria Paula Sassoli Fazan, M.D., Ph.D., Associate Professor, Department of Surgery and Anatomy, School of Medicine of Ribeirao Preto, USP, Av. Bandeirantes 3900, Ribeirao Preto, SP, Brazil, 14049-900, Tel: +55 16 3602-4634; Fax: +55 16 3633-0017; E-mail: vpsfazan@yahoo.com.br; vpsfazan@gmail.com

Rec date: Apr 14, 2014, **Acc date:** May 23, 2014, **Pub date:** May 25, 2014

Abstract

Anatomical and physiological aspects involving rats and mice have shown similarities and differences between these experimental animal models. In cardiovascular physiology research, rats are being substituted by mice since mice are more susceptible to genetic manipulation. Nevertheless, little is known about mice normal anatomy and/or physiology to allow the correct interpretation of altered responses on genetically manipulated animals. We compared morphometric ultrastructural parameters of the aortic depressor nerve (ADN) and extrinsic renal nerve (SRN) between Wistar rats and C57BL/6J mice. After spontaneous activity recordings together with the arterial pressure pulse, ADN and SRN were dissected and prepared for light and transmission electron microscopy. Morphometry was performed with an image analysis software and took into consideration the fascicle area and diameter, myelinated and unmyelinated fiber number, density, area and diameter, myelin sheath area and the g-ratio. Comparisons were made for the same nerve between mice and rats and differences were considered significant when $p<0.05$. Both nerves were large in rats compared to mice, as were the myelinated fibers. On the other hand, unmyelinated fibers density, size and distributions were not different between species. These results suggest physiological differences on the fast conduction fibers between species, with possible different functional role. Morphological comparisons of the quantitative composition of peripheral nerves in different species and strains are very rare. Our study contributes to a morphological understanding of important nerves related to cardiovascular reflexes in two animal models. It also presents, for the first time, ultrastructural morphometric characteristics of the ADN in mice. This data provide a morphological basis for further studies involving functional investigations for reflex regulation of circulation in experimental model of hypertension and to improved cardiovascular system knowledge.

Keywords: Extrinsic renal nerves; Aortic depressor nerves; Wistar rats; C57BL/6J mouse; Morphology; Ultrastructure

Introduction

Reflex regulation of the circulation involving afferent nerves within the cardiovascular system has been widely investigated. The aortic depressor nerves (ADN) and extrinsic renal nerves (SRN) role in these reflexes have been stimulated and/or recorded in diverse experimental models [1-4]. The ADN are important baroreceptor afferences responsible for cardiovascular regulation, contributing for maintenance of the rapid changes in blood pressure, cardiovascular variability as well as modulation of central sympathetic outflow [5-7]. The ADN morphology has been studied extensively in rats [8-10], cats [11,12] and rabbits [13,14], but information on the structure of this nerve has not been reported in mice.

The SRN are constituted by afferent and efferent sympathetic nerve fibers that play a role on maintenance of renal function. An adequate renal function in turn, contributes to control of cardiovascular homeostasis in the longer term. In addition, the renal nerves play an important role in renal reflexes, being involved not only in renal regulation but also in cardiovascular regulation [15-17]. Sustained changes in renal sensory receptors and conducted via renal afferent nerves modify efferent sympathetic nerve activity with consequences for arterial pressure [18,19]. Despite this functional importance, there are few morphological studies on extrinsic renal nerves in different species [20-24].

In addition, anatomical comparisons between rats and mouse have shown important differences between these experimental animal models in peripheral nerves [25]. The introduction of the genetically manipulated mice brought up the need for a throughout understanding of this species normal morphology and function, to allow the correct interpretation of findings regarding the genetic alterations. Much of the normal physiology, as well as morphological aspects well established for other species, remain unknown for the mouse.

This study describes the normal ultrastructure and morphometry of the ADN and the SRN in rats and mice, and compare the findings between the two species, discussing their physiological role.

Materials and Methods

This study was approved by the Institutional Ethics Committee for Animal Research (CETEA–Comitê de Ética em Experimentacao Animal, protocol number 001/2004)., following the Guidelines for the Care and Use of Laboratory Animals prepared by the National Academy of Sciences and published by the National Institute of Health (Copyright © 2011 by the National Academy of Sciences). Every effort was made to minimize the suffering and the number of the animals used. All animals had *ad libitum* access to pelleted food for rodents and tap water throughout the experiments.

Experiments were performed on male adult Wistar rats (N=7) and male adult C57BL/6J mice (N=6). Animals were weighed, anesthetized with sodium pentobarbital (Nembutal, Abbott Laboratories, Illinois; 40 mg/Kg, i.p.), and placed on a surgical table in dorsal decubitus. The animals were submitted to a cervicotomy and the left aortic depressor nerve (ADN), when present as an isolated strand, was placed on a bipolar steel electrode for its spontaneous activity recording, simultaneously with the arterial pressure pulse. A catheter was inserted into the right carotid artery and connected to a pressure transducer (Statham PB23Gb) for direct measurement of arterial pressure (AP) (for details, see refs. 8 and 9). After this first step, animals were carefully turned to a right lateral decubitus and the left extrinsic renal nerve (SRN) was identified and exposed by a left flank incision using a retroperitoneal approach. The main branch originating from the aorticorenal ganglion leading to the kidney was carefully isolated using a dissecting microscope. Likewise for the ADN, renal nerve activity and blood pressure recordings were performed synchronously to confirm the presence of characteristics renal sympathetic nerve activity, allowing the correct identification of the SRN before morphological studies [22,23].

After the recordings, the ADN (N=7 for rats and N=6 for mice) and SRN (N=6 for rats and N=5 for mice) were removed and prepared for histological studies as previously described [8,9,22,23]. During the dissection process, two renal nerves (one from rat and one from mouse) were damaged and withdrawn from the study. All the nerve segments were processed at once so that they were submitted to absolutely the same experimental conditions throughout the histological procedures.

For the light microscopy study, both nerves were oriented to permit semi-thin (0.5 to 1.0 μm) transverse sections of the fascicles, which were stained with 1% toluidine blue and observed under the oil immersion lens of an Axiophot photomicroscope (Carl Zeiss, Jena, Germany). With an image analysis software (KS400, Kontron 2.0, Eching Bei Müchen, Germany), morphometric parameters of the fascicles, myelinated fibers and respective axons of all nerves were obtained [26,27]. The area and diameter were measured for each fascicle (excluding perineurium) and for each myelinated fiber visible on the endoneural space. For each nerve with two or more fascicles, the total fascicular area was obtained by summing the areas of the two individual fascicles. Hereafter, the term fascicular area will be used as a synonym of total fascicular area. All myelinated fibers present in the endoneural space were counted and the myelinated fiber density was calculated. For the myelinated axons, both axonal diameter (defined by the inner limit of the myelin lamellae) and fiber diameter (defined by the outer limit of the myelin lamellae) were measured and the myelin sheath area (defined by the inner and outer limit of the myelin lamellae) was automatically calculated for each myelinated fiber [26,27]. The ratio between the axon diameter and the fiber diameter, the g-ratio (an index of axonal axonal atrophy), was obtained [28,29] for each myelinated fiber. Also, the percentage of the total fascicular area occupied by the myelinated fibers was calculated and hereafter will be referred as myelinated fiber percentage of occupancy.

For the transmission electron microscopy studies, transversal ultra-thin sections (40 nm thick) were mounted on 2 x 1 slot grids, covered with formvar 0.5% solution, stained with lead citrate and uranyl acetate, and visualized using the transmission electron microscope (JEM-1230, JEOL-USA, Inc., Peabody, MA, USA), equipped with a digital camera. The endoneural space of all nerves was fully scanned without overlap of the microscopic fields [30,31,32] and images were digitalized to an IBM-PC hard drive. Sample morphometry was not used and 100% of the fascicle area was studied. Using the image analysis software (KS-400), the total number of the unmyelinated fibers was counted, and their area and diameter were measured. The density of the unmyelinated fiber was calculated and the ratio between myelinated/unmyelinated fibers was determined. The percentage of the fascicular area occupied by the unmyelinated fibers (unmyelinated fiber percentage of occupancy) was also calculated.

Histograms of diameter distribution of unmyelinated fibers and myelinated fibers, respective axons were constructed. Histograms were also constructed for the g-ratio distributions of the myelinated fibers. For mice myelinated fibers, one histogram of all fibers present in all nerves studied was used due a relatively smaller number of myelinated fibers. Histograms for the myelinated fibers and axons distributions were separated into class intervals increasing by 0.5 μm while for the g-ratio histograms they were separated into class intervals increasing by 0.1 μm. Unmyelinated fiber distribution histograms were constructed into class intervals increasing by 0.1 μm.

For the statistical analysis, mice and rat data from the same nerve (ADN or SRN) were compared. Data were tested for normal distribution by the Kolmogorov-Smirnov test followed by the Levene test for variance equivalence. Differences between nerves were evaluated by unpaired t-test for normally distributed data. Nonparametric data were compared by the Mann-Whitney test. Histograms were compared by the One Way ANOVA on ranks, followed by the *post-hoc* test of Dunn, provided that all data were nonparametric. Differences were considered significant if $p<0.05$. Data are expressed as mean ± SEM (standard error of mean).

Results

Adult rats were heavier (295 ± 13 g) than adult mice (25 ± 0.6 g), with a difference about 12 times between them ($p<0.001$).

A single fascicle was observed on all aortic depressor nerves from rats and in 83% of mice (1 out of 6) (Figure 1) being the epineurium constituted by loose longitudinally oriented collagen fibers, blood vessels and fat tissue in both species. The perineurium is characterized by lamellae of flattened cells separated by thin layers of collagen fibers, and the endoneural space presents myelinated and unmyelinated axons, intermingled with fibroblasts, collagen fibers, blood vessels and Schwann cells. Endoneural blood vessels were not found in all ADN, being present in 67% of mice and 43% of rats.

All SRN of mice consisted of a single fascicle, while in rats, one nerve with two fascicles was found (Figure 1). Renal nerves from both species presented similar features of the ADN epi-and perineurium. The endoneural space of the renal nerves was filled mostly by unmyelinated axons but the other elements present in the ADN endoneural space were also present in the SRN. Endoneural blood

vessels were not found in all SRN from mice while 67 % of these nerves in rats showed one single endoneural capillary vessel. One interesting morphological feature that was found only in the SRN either in rats or in mice was the presence of a neuronal cell body in the endoneural space (Figure 1). This was not seen in the ADN.

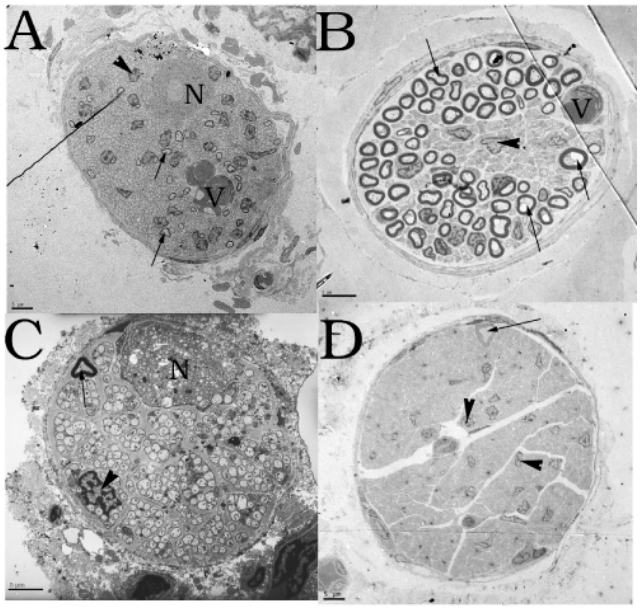

Figure 1: Representative thin cross sections of the aortic depressor nerve (ADN) (A and B) and the sympathetic renal nerve (C and D) from mice (A and C) and rats (B and D). All nerves shown are monofasciculated. ADN present a larger number of myelinated fibers (arrows) than the SRN. Some mice nerves presented a neuronal cell body (N) in the endoneural space. This was not observed in rats. Endoneural blood vessels (V) and Schwann cell nuclei (arrowheads) are indicated in the endoneural space. Bar=5 μm

Fascicle Morphometry

Table 1 shows the average values for fascicular morphometric parameters of the ADN from rats and mice. Mice ADN contained on average 1131 ± 101 fibers (range of 779 to 1377; 2% myelinated and 98% unmyelinated), while rat nerves contained 356 ± 76 fibers (range of 145 to 567; 23% myelinated and 77% unmyelinated). As expected, the fascicular area and diameter were larger in rats compared to mice (p=0.001). Similarly, the myelinated fiber number was higher in rats than mice (p=0.001). In contrast, the unmyelinated fiber number in mice was larger than rats (p=0.001). Myelinated and unmyelinated fiber densities were larger in mice compared to rats (p=0.03 and p=0.001, respectively). The unmyelinated to myelinated fibers ratios were also higher in mice (p=0.001).

Table 2 shows the average values for fascicular morphometric parameters for the SRN in rats and mice. Mice SRN contained on average 670 ± 200 fibers (range of 380 to 832; 0.6% myelinated and 99.4% unmyelinated), while rat nerves contained 1258 ± 280 fibers (range of 939 to 1706; 1.7% myelinated and 98.3% unmyelinated). As for the ADN, rats showed larger fascicles and number of fibers compared to mice (p<0.05), except for the myelinated and unmyelinated fibers densities, that showed similar values. Also, the statistical analysis did not show differences between the unmyelinated/myelinated fibers ratio in the SRN between species.

Fascicle parameter	C57BL/6J mouse	Wistar rats
Fascicular area (μm^2)	159 ± 16	1024 ± 101*
Fascicular diameter (μm)	13 ± 0.9	30 ± 2*
Myelinated fiber number	24 ± 4	81 ± 9*
Unmyelinated fiber number	1106 ± 102	275 ± 65*
Myelinated fiber density (fiber/mm^2)	0.16 ± 0.03	0.08 ± 0.01*
Unmyelinated fiber density (fiber/μm^2)	7.1 ± 0.6	0.3 ± 0.1*
Unmyelinated/myelinated ratio	66 ± 25	4 ± 0.9*

Table 1: Average fascicular parameters from the aortic depressor nerves (ADN) in adult C57BL/6J mice and Wistar rats. * indicates significant difference between groups

Fascicle parameter	C57BL/6J mouse	Wistar rats
Fascicular area (μm^2)	781 ± 106	5027 ± 1484*
Fascicular diameter (μm)	37 ± 4	85 ± 18*
Myelinated fiber number	4 ± 2	22 ± 10*
Unmyelinated fiber number	666 ± 89	1236 ± 115*
Myelinated fiber density (fiber/mm^2)	4969 ± 1772	4677 ± 1829
Unmyelinated fiber density (fiber/μm^2)	0.9 ± 0.1	0.7 ± 0.1
Unmyelinated/myelinated ratio	306 ± 130	109 ± 26

Table 2: Average fascicular parameters from the sympathetic renal nerves (SRN) in adult C57BL/6J mice and Wistar rats. * indicates significant difference between groups

Fiber Morphometry

The average areas of the myelinated fibers and respective axons and myelin sheaths for depressor and renal nerves are shown in Figure 2. All values were higher in rats compared to mice for both nerves, without attaining statistical significance on the myelinated axon area on the renal nerves. Myelinated fiber diameter of the ADN showed an average of 1.5 ± 0.1 μm for mice (range of 1.2-1.7 μm) and 2.0 ± 0.1 μm (range of 1.6-2.4 μm) for rats, being significantly larger in rats (p=0.001), with a difference of 26.6% between them. For the SRN, the values were 3.2 ± 0.4 μm (range of 1.4-7.4 μm) for mice and 3.4 ± 0.2 μm (range of 1.6-10.5 μm) for rats, with no significant difference. Myelinated axons average diameter was 0.85 ± 0.05 μm (range of 0.61-0.97 μm) for mice and 1.10 ± 0.05 μm (range of 0.90-1.34 μm) for rats in ADN with a difference of 23% between the two species (p=0.007). For the SRN, averages were 2.19 ± 0.29 μm (range of 0.8-5.7 μm) for mice and 1.85 ± 0.10 μm (range of 0.9-7.1 μm) for rats, with no statistical difference.

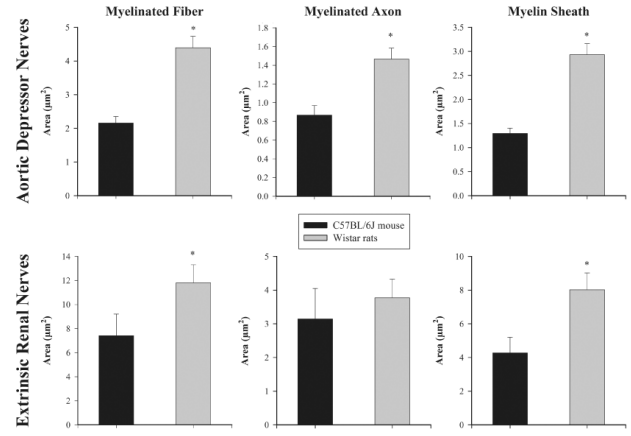

Figure 2: Average area of the myelinated fibers and respective axons and myelin sheath in the aortic depressor nerve (ADN) and sympathetic renal nerve (SRN) from Wistar rats (grey filled bars) and C57BL/6J mice (black filled bars). Average values are larger in rats compared to mice. *indicates significant difference between animal species.

The average values for unmyelinated fiber area of ADN was 0.39 ± 0.02 μm^2 for mice (range of 0.32-0.45 μm^2) and 0.31 ± 0.04 μm^2 for rats (range of 0.24-0.52 μm^2), with no differences between them. For the SRN, unmyelinated fibers average area was 0.41 ± 0.01 μm^2 (range of 0.39-0.43 μm^2) for mice and 0.49 ± 0.08 μm^2 (range of 0.27-0.79) for rats, also with no significant difference.

Histograms of size distribution of the myelinated fibers showed that mice fiber distributions were shifted to the left compared to rats in both, depressor and renal nerves (Figure 3). The histograms of g-ratio distribution were unimodal, with peaks between 0.6-0.7 in both nerves from both animal species. The g-ratio values for mice ADN ranged from at 0.4-0.8 while in rats it ranged from 0.3-0.9. For the SRN g-ratio values ranged from 0.5-0.8 in mice and 0.4-0.9 in rats. The g-ratio distributions showed no differences between species for both nerves.

Figure 4 shows the size distributions histograms for unmyelinated fibers for depressor and renal nerves in rats and mice. In mice, ADN unmyelinated fiber distribution ranged from 0.1 to 1.9 μm, with a peak at 0.5 μm. In rats, the unmyelinated fibers of the ADN ranged from 0.1 to 1.1 μm, also with a peak at 0.5 μm. The SRN unmyelinated fibers diameter in mice ranged from 0.2 to 1.8 μm, with a peak at 0.8 μm while in rats the diameters ranged from 0.1 to 1.6 μm, with a flat plateau between 0.5-0.7 μm. No differences were found on the unmyelinated fibers distributions between species for both nerves.

Discussion

Our study contributes to a morphological understanding of important nerves related to cardiovascular reflexes in two animal models. It also presents, for the first time, ultrastructural morphometric characteristics of the ADN in mice.

Aortic depressor nerve in rats and mice

The comparison between mice and rat ADN size showed that these nerves are much smaller in mice. This would be expected due to a proportional difference on the animals' size. This difference was also present on the myelinated fiber numbers. Interestingly, the proportions between animals' sizes, nerves sizes and myelinated fiber numbers were decrescent since rats were 12 times heavier than mice while ADN from rats were 7 times larger than mice but had only 3 times more myelinated fibers. In line with these results the ADN myelinated fibers sizes (area and diameter) were smaller in mice.

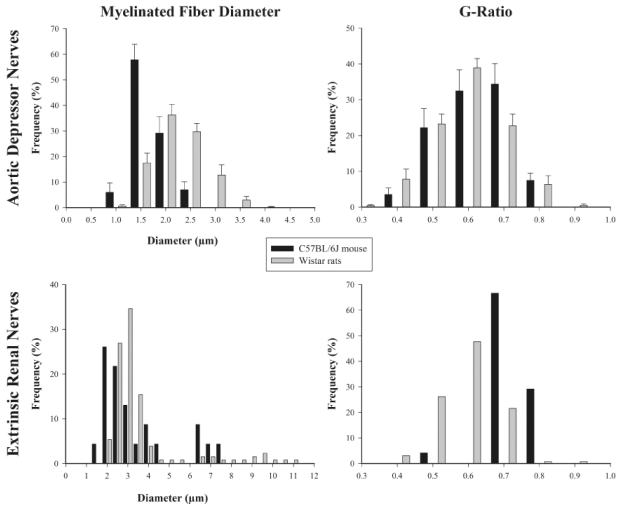

Figure 3: Size distribution histograms of the myelinated fibers and respective g-ratio in the aortic depressor nerve (ADN) and sympathetic renal nerve (SRN) from Wistar rats (grey filled bars) and C57BL/6J mice (black filled bars). For the ADN, average values from each nerve studied are shown, with standard error of means (SEM). For mice, the total number of fibers from all nerves is shown. No morphometric differences were observed between animal species.

The ADN myelinated fibers are the fast conducting fibers of the baroreflex, and their normal electrophysiological characteristics were well described in rats more than three decades ago [33]. The normal baroreflex in mice was recently investigated [34]. It is widely known that conduction velocity of a myelinated fiber can be estimated taking into consideration their morphometric parameters, particularly fiber diameter and axon diameter [35]. In the present study, we did not measure the conduction velocity of the nerves but, using the scaling factor of Boyd and Kalu [36] for computing the corresponding value for small myelinated fibers (4.6 times total fiber diameter), we may speculate that the ADN myelinated axons in rats conduct at 7.3 to 11.0 m/s and those in mice at 5.5 to 7.8 m/s. Despite little overlap between values, there is no indication that mice would have a poor baroreflex control of the arterial pressure compared to rats. These differences are probably due to the animal size because in mice the distance from the receptors to the central nervous system is smaller than in rats. Thus, it is not necessary for mice to have large faster conduction myelinated fibers, confirming that the neural systems adapt to requirements of animal size [37]. This hypothesis is confirmed by the g-ratio average values and distributions where there were no different between species. Rushton [28] found that when g-ratio equals 0.6, the relationship is theoretically optimal for the spread of current from one node of Ranvier to the next, being the myelinated fiber able to conduct

at maximum speed and average g-ratio values for both species were 0.6.

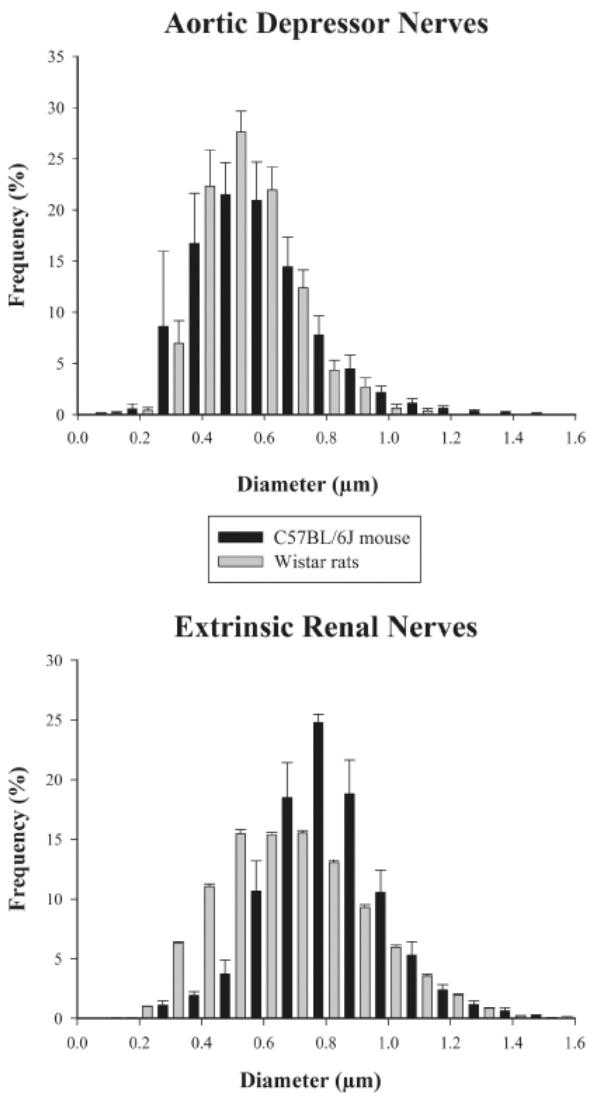

Figure 4: Size distribution histograms of the unmyelinated fibers in the aortic depressor nerve (ADN) and sympathetic renal nerve (SRN) from Wistar rats (grey filled bars) and C57BL/6J mice (black filled bars). No morphometric differences were observed between animal species. Bars represent mean ± SEM.

The unmyelinated fiber number of the ADN was larger (4 times) in mice compared to rats. The ratio between unmyelinated and myelinated fibers is considered ideal when it is equal to a minimum of 3:1 [38,39]. The unmyelinated-to-myelinated fiber ratio was 4:1 for rats and 66:1 for mice. Unmyelinated fibers in the ADN of rats were described to contribute significantly to the inhibition of the vasomotor medullary centers [40] and their discharges during normotension are sparse, especially from those fibers with irregular activity [40]. When these baroreceptor unmyelinated fibers are stimulated electrically, powerful depressor reflexes are evoked for control blood pressure [40]. Also, electrical stimulation of these unmyelinated fibers (type C) promotes a sympatho-inhibitory action on renal and cardiac nerve activities, having the unmyelinated fibers a greater depressor effect [41]. Thus, they are considered as baroreceptor fibers and it is a literature consensus that rat ADN present very few chemoreceptos fibers, if any [42,43]. No information about number, size, electrophysiological characteristics or function of mice ADN unmyelinated fibers is available. The carotid sinus nerves in rats (a nerve well known to contain chemoreceptor fibers) contain 83% of unmyelinated fibers distributed unimodaly, with diameters ranging from 0.2 to 1.7 µm (average of 0.78 µm) [44]. This is very similar to the observations in our study for mice ADN and might be a suggestion that some of these unmyelinated fibers have a chemoreceptor role. Despite the number differences, unmyelinated fibers sizes and distributions did not differ between species, suggesting no differences in the conduction velocity of these fibers. Morphometric data shown in this study are similar to previous ones for the rat ADN [8] but are being described for the first time in mice.

Sympathetic renal nerve in rats and mice

Similarly to the ADN, the SRN is smaller in mice, as are the myelinated fiber number and sizes. This is in line with differences in animals sizes already discussed for the ADN. The SRN myelinated fibers are considered to be sensory afferents [18,20] and they transmit afferent impulses from intra-renal mechanoreceptors and chemoreceptors to the central nervous system [45-48]. Differences in fiber numbers can also be related to the animal size; since mice kidneys are smaller, the sensory area to be covered by afferent fibers is smaller and fewer fibers are necessary. Again, larger myelinated fiber sizes (area and diameter) in rats indicate that a higher conduction velocity is necessary in these animals so the impulse will reach the central nervous system on a timely way for the necessary information. Nevertheless, g-ratio average and distributions are in accordance to the optimal values described for the maximum conduction velocity [28] in both rats and mice.

For the unmyelinated fibers, despite differences in numbers (larger in rats), no differences were found on their density (fiber number per nerve area), average size (area and diameter) and size distributions. This is a morphological indication that unmyelinated fibers in the SRN of rats and mice might present a similar physiological role. Although the majority of unmyelinated fibers are sympathetic efferents, the afferent innervation is also primarily unmyelinated [18,49-52]. Barajas and Wang [53] suggested that unmyelinated fibers are primary efferent and act directly on regulation of renal function [54].

For the renal nerves, morphometric results presented here are quite similar those described in literature [22,23] for rats and mice. Nevertheless, the systematic comparison between the two is being present for the first time.

Conclusion

The understanding of morphologic and morphometric parameters is important because of the direct relations between them and nerve function, particularly the conduction velocity. This study provides the morphological basis for further studies involving ADN and SRN functions, especially when animal models of diseases are under investigation.

Acknowledgements

We thank Mr. Antônio Renato Meirelles e Silva, Experimental Neurology Laboratory and Ms. Maria Tereza P. Maglia, Electron Microscopy Laboratory, School of Medicine of Ribeirão Preto, for excellent technical support. Grant sponsor: FAPESP (Fundação de Amparo à Pesquisa do Estado de São Paulo); Grant numbers: 2012/00321-0 and 2013/01111-0; **Grant sponsor:** CNPq (Conselho Nacional de Pesquisa e Tecnologia); **Grant number:** 300900/2013-9. There is no conflict of interest.

References

1. Coote JH, Sato Y (1977) Reflex regulation of sympathetic activity in the spontaneously hypertensive rat. Circ Res 40: 571-577.
2. Morilak DA, Morris M, Chalmers J (1988) Release of substance P in the nucleus tractus solitarius measured by in vivo microdialysis: response to stimulation of the aortic depressor nerves in rabbit. Neurosci Lett 94: 131-137.
3. Gava AL, Balarini CM, Peotta VA, Abreu GR, Cabral AM, et al. (2012) Baroreflex control of renal sympathetic nerve activity in mice with cardiac hypertrophy. Auton Neurosci 170: 62-65.
4. Santana-Filho V, Davis GJ, Castania JA, Ma X, Salgado HC, et al. (2014) Autocrine/paracrine modulation of barorreceptor activity after antidromic stimulation of aortic depressor nerve in vivo. Auton Neurosci 180: 24-31.
5. Lanfranchi PA, Somers VK (2002) Arterial baroreflex function and cardiovascular variability: interactions and implications. Am J Physiol Regul Integr Comp Physiol 283: R815-826.
6. Schultz HD, Li YL, Ding Y (2007) Arterial chemoreceptors and sympathetic nerve activity: implications for hypertension and heart failure. Hypertension 50: 6-13.
7. Kirkman E, Sawdon M (2010) Neurological and humoral control of blood pressure. Anaesth Intens Care Med 11: 159-164.
8. Fazan VP, Salgado HC, Barreira AA (1997) A descriptive and quantitative light and electron microscopy study of the aortic depressor nerve in normotensive rats. Hypertension 30: 693-698.
9. Fazan VPS, Fazan Jr R, Salgado HC, Barreira AA (1999) Morphology of aortic depressor nerve myelinated fibers in normotensive Wistar-Kyoto and spontaneously hypertensive rats. J Auton Nerv Syst 77: 133-139.
10. Fazan VP, Salgado HC, Barreira AA (2001) Aortic depressor nerve unmyelinated fibers in spontaneously hypertensive rats. Am J Physiol Heart Circ Physiol 280: H1560-1564.
11. AGOSTONI E, CHINNOCK JE, DE DALY MB, MURRAY JG (1957) Functional and histological studies of the vagus nerve and its branches to the heart, lungs and abdominal viscera in the cat. J Physiol 135: 182-205.
12. DEVANANDAN MS (1964) A STUDY OF THE MYELINATED FIBRES OF THE AORTIC NERVE OF CATS. J Physiol 171: 361-367.
13. Sarkar BB (1922) The depressor nerve of the rabbit. Proc R Soc B 93: 230-234.
14. Nonidez JF (1935) The aortic (depressor) nerve and its associated epithelioid body, the glomus aorticum. Am J Anatomy 57: 259-301.
15. Schramm LP, Strack AM, Platt KB, Loewy AD (1993) Peripheral and central pathways regulating the kidney: a study using pseudorabies virus. Brain Res 616: 251-262.
16. DiBona GF (2003) Neural control of the kidney: past, present, and future. Hypertension 41: 621-624.
17. Katholi RE, Rocha-Singh KJ (2009) The role of renal sympathetic nerves in hypertension: has percutaneous renal denervation refocused attention on their clinical significance? Prog Cardiovasc Dis 52: 243-248.
18. DiBona GF, Kopp UC (1997) Neural control of renal function. Physiol Rev 77: 75-197.
19. Grisk O, Rettig R (2004) Interactions between the sympathetic nervous system and the kidneys in arterial hypertension. Cardiovasc Res 61: 238-246.
20. Niijima A (1975) Observation on the localization of mechanoreceptors in the kidney and afferent nerve fibres in the renal nerves in the rabbit. J Physiol 245: 81-90.
21. DiBona GF, Sawin LL, Jones SY (1996) Differentiated sympathetic neural control of the kidney. Am J Physiol 271: R84-R90.
22. Fazan VP, Ma X, Chapleau MW, Barreira AA (2002) Qualitative and quantitative morphology of renal nerves in C57BL/6J mice. Anat Rec 268: 399-404.
23. Sato KL, do Carmo JM, Fazan VP (2006) Ultrastructural anatomy of the renal nerves in rats. Brain Res 1119: 94-100.
24. Sato KL, Sanada LS, Ferreira Rda S, de Marco MC, Castania JA, et al. (2014) Renal nerve ultrastructural alterations in short term and long term experimental diabetes. BMC Neurosci 15: 5.
25. Rigaud M, Gemes G, Barabas ME, Chernoff DI, Abram SE, et al. (2008) Species and strain differences in rodent sciatic nerve anatomy: implications for studies of neuropathic pain. Pain 136: 188-201.
26. Jeronimo A, Jeronimo CA, Rodrigues Filho OA, Sanada LS, Fazan VP (2005) Microscopic anatomy of the sural nerve in the postnatal developing rat: a longitudinal and lateral symmetry study. J Anat 206: 93-99.
27. Jeronimo A, Jeronimo CA, Rodrigues Filho OA, Sanada LS, Fazan VP (2008) A morphometric study on the longitudinal and lateral symmetry of the sural nerve in mature and aging female rats. Brain Res 1222: 51-60.
28. RUSHTON WA (1951) A theory of the effects of fibre size in medullated nerve. J Physiol 115: 101-122.
29. Smith RS, Koles ZJ (1970) Myelinated nerve fibers: computed effect of myelin thickness on conduction velocity. Am J Physiol 219: 1256-1258.
30. Fazan VP, Rodrigues Filho OA, Jordão CE, Moore KC (2009) Ultrastructural morphology and morphometry of phrenic nerve in rats. Anat Rec (Hoboken) 292: 513-517.
31. Fazan VP, Rodrigues Filho OA, Jordão CE, Moore KC (2009) Phrenic nerve diabetic neuropathy in rats: unmyelinated fibers morphometry. J Peripher Nerv Syst 14: 137-145.
32. Oliveira FS, Nessler RA, Castania JA, Salgado HC, Fazan VP (2013) Ultrastructural and morphometric alterations in the aortic depressor nerve of rats due to long term experimental diabetes: effects of insulin treatment. Brain Res 1491: 197-203.
33. Brown AM, Saum WR, Tuley FH (1976) A comparison of aortic baroreceptor discharge in normotensive and spontaneously hypertensive rats. Circ Res 39: 488-496.
34. Rodrigues FL, de Oliveira M, Salgado HC, Fazan R Jr (2011) Effect of baroreceptor denervation on the autonomic control of arterial pressure in conscious mice. Exp Physiol 96: 853-862.
35. Gillespie MJ, Stein RB (1983) The relationship between axon diameter, myelin thickness and conduction velocity during atrophy of mammalian peripheral nerves. Brain Res 259: 41-56.
36. Boyd IA, Kalu KU (1979) Scaling factor relating conduction velocity and diameter for myelinated afferent nerve fibres in the cat hind limb. J Physiol 289: 277-297.
37. Purves D, Rubin E, Snider WD, Lichtman J (1986) Relation of animal size to convergence, divergence, and neuronal number in peripheral sympathetic pathways. J Neurosci 6: 158-163.
38. Ochoa J, Mair WG (1969) The normal sural nerve in man. I. Ultrastructure and numbers of fibres and cells. Acta Neuropathol 13: 197-216.
39. Friede RL, Beuche W (1985) Combined scatter diagrams of sheath thickness and fibre calibre in human sural nerves: changes with age and neuropathy. J Neurol Neurosurg Psychiatry 48: 749-756.
40. Thorén P, Saum WR, Brown AM (1977) Characteristics of rat aortic baroreceptors with nonmedullated afferent nerve fibers. Circ Res 40: 231-237.
41. Numao Y, Siato M, Terui N, Kumada M (1985) The aortic nerve-sympathetic reflex in the rat. J Auton Nerv Syst 13: 65-79.
42. Sapru HN, Krieger AJ (1977) Carotid and aortic chemoreceptor function in the rat. J Appl Physiol Respir Environ Exerc Physiol 42: 344-348.

43. Kobayashi M Cheng ZB, Tanaka K, Nosaka S (1999) Is the aortic depressor nerve involved in arterial chemoreflexes in rats? J Auton Nerv Syst 78: 38-48.
44. McDonald DM (1983) Morphology of the rat carotid sinus nerve. II. Number and size of axons. J Neurocytol 12: 373-392.
45. Zimmermann HD (1975) Myelinated nerve fibers in the rat kidney. Light- and electron microscopic studies. Cell Tissue Res 160: 485-493.
46. Calaresu FR, Stella A, Zanchetti A (1976) Haemodynamic responses and renin release during stimulation of afferent renal nerves in the cat. J Physiol 255: 687-700.
47. Simon OR, Schramm LP (1984) The spinal course and medullary termination of myelinated renal afferents in the rat. Brain Res 290: 239-247.
48. Gattone VH 2nd, Marfurt CF, Dallie S (1986) Extrinsic innervation of the rat kidney: a retrograde tracing study. Am J Physiol 250: F189-196.
49. Barajas L, Müller J (1973) The innervation of the juxtaglomerular apparatus and surrounding tubules: a quantitative analysis by serial section electron microscopy. J Ultrastruct Res 43: 107-132.
50. Barajas L, Powers K, Wang P (1984) Innervation of the renal cortical tubules: a quantitative study. Am J Physiol 247: F50-60.
51. Barajas L, Powers K, Wang P (1985) Innervation of the late distal nephron: an autoradiographic and ultrastructural study. J Ultrastruct Res 92: 146-157.
52. Barajas L, Powers KV (1988) Innervation of the thick ascending limb of Henle. Am J Physiol 255: F340-348.
53. Barajas L, Wang P (1978) Myelinated nerves of the rat kidney. A light and electron microscopic autoradiographic study. J Ultrastruct Res 65: 148-162.
54. DiBona GF (2001) Functionally specific renal sympathetic nerve fibers: role in cardiovascular regulation. Am J Hypertens 14: 163S-170S.